Neutron star matter with strange interactions within constraints by GW170817 in a relativistic quark model

Himanshu S. Sahoo,[1] Rabindranath Mishra,[1] Deepak K. Mohanty,[1] Prafulla K. Panda,[2] and Niranjan Barik[2]
[1]*Department of Physics, Ravenshaw University, Cuttack 753 003, India*
[2]*Department of Physics, Utkal University, Bhubaneswar 751 004, India*

(Received 7 February 2019; published 6 May 2019)

The effect of strange interactions in neutron star matter and the role of the strange meson-hyperon couplings are studied in a relativistic quark model where the confining interaction for quarks inside a baryon is represented by a phenomenological average potential in an equally mixed scalar-vector harmonic form. The hadron-hadron interaction in nuclear matter is then realized by introducing additional quark couplings to σ, ω, ρ, σ^*, and ϕ mesons through mean-field approximations. The meson-baryon couplings are fixed through the SU(6) spin-flavor symmetry and the SU(3) flavor symmetry to determine the hadronic equation of state (EoS). We find that the SU(3) coupling set gives the potential depth between Λ's around -5 MeV and favors a stiffer EoS. Using the stiffest EoS from the SU(3) we determine the tidal Love number k_2, the tidal deformability λ, and the dimensionless tidal deformability Λ_D. We obtain a value of $\Lambda_D = 483$ corresponding to a $1.4M_\odot$ star while the weighted tidal deformability $\widetilde{\Lambda} = 624$ for a symmetric binary system of chirp mass $\mathcal{M} = 1.188M_\odot$. The radius for the canonical neutron star is found to be 13.1 km.

DOI: 10.1103/PhysRevC.99.055803

I. INTRODUCTION

The recent observation of gravitational waves from a binary neutron star coalescence by the Advanced LIGO and Virgo gravitational wave detectors, i.e., event GW170817 [1], has provided new insight on the maximum mass as well as the radii distribution of neutron stars [2–6]. Studies based on the GW170817 observation have put forth a stringent limit on the radius corresponding to a $1.4M_\odot$ mass neutron star, between $9.9 < R_{1.4} < 13.6$ km. Such a limit sets a strong constraint on the equation of state (EoS) of dense matter. The EoS plays a crucial role in determining the composition of dense matter relevant to neutron stars, the relation between the mass and radius of neutron stars, as well as other macroscopic properties such as the tidal deformability and stellar moment of inertia. In particular, limits have been set on the dimensionless deformability parameter Λ_D and the combined dimensionless tidal deformability $\widetilde{\Lambda}$ of the binary system. The value [1] for $\Lambda_D(1.4M_\odot)$ has been restricted to $\Lambda_D(1.4M_\odot) \leqslant 800$ while the limit on $\widetilde{\Lambda}$ has been updated [7] to $70 \leqslant \widetilde{\Lambda} \leqslant 720$.

In light of such recent advances in multimessenger observations and the availability of precise observational data, the composition of neutron stars can be modeled so as to lie within the new constraints. The composition of dense matter relevant to neutron stars consists not only of nucleons and leptons but also several exotic components such as hyperons, mesons as well as quark matter in different forms and phases. Since very high density is energetically favorable for the creation of particles with strange content, it is expected that hyperons may appear in the inner core of neutron stars at densities 2–3 times the normal saturation density $\rho_0 = 0.15\,\mathrm{fm}^{-3}$. The onset of this new degree of freedom softens the EoS and lowers the maximum mass [8–11], leading to the *hyperon puzzle*. In the present work we study the properties of isolated and binary neutron stars with strange interactions within a relativistic quark model, alternatively called the modified quark meson coupling model (MQMC) [12–15]. The MQMC model is based on a confining relativistic independent quark potential model rather than a bag to describe the baryon structure in vacuum. In such a picture the quarks inside the baryon are considered to be independently confined by a phenomenological average potential with an equally mixed scalar-vector harmonic form. Such a potential has characteristically simplifying features in converting the independent quark Dirac equation into a Schrödinger-like equation for the upper component of Dirac spinor, which can be solved easily. The implications of such potential forms in the Dirac framework have been studied earlier [16,17].

In an earlier work [14] we studied hyperon stars in the MQMC model where the baryon-baryon interaction was realized through σ, ω, and ρ meson exchanges and the strange quarks were considered as spectators. Recently, this model was applied for the study of properties of Λ and Ξ^0 hypernuclei [18] as well as in developing an EoS [19] within the constraints set by GW170817 event. In the present attempt we incorporate an additional pair of hidden strange mesons σ^* and ϕ [20] which couple only to the strange quark and the hyperons of nuclear matter. The relevant parameters of the interaction are obtained self-consistently by realizing the saturation properties such as binding energy and pressure. The hyperon couplings to the strange mesons are quite uncertain. In the present work we tried with three different sets: first with SU(6) spin flavor symmetry [21], the second one by using the available hyperon-nucleon interaction potential at saturation

density for the Λ, Σ, and Ξ hyperons to $U_\Lambda = -28$ MeV, $U_\Sigma = 30$ MeV, and $U_\Xi = -18$ MeV respectively to determine the hyperon couplings to the vector ω meson [14], and the third one with SU(3) symmetry [22] where couplings are expressed in terms of the mixing angle θ_v. The main objective in the consideration of such sets is to get the neutron star's maximum mass. We observe that the SU(3) coupling set gives a massive neutron star. To add a greater credence to our choice of SU(3), we determine the tidal deformability and moment of inertia of hyperonic stars within the MQMC framework.

The paper is organized as follows: In Sec. II, a brief outline of the model describing the baryon structure in vacuum is discussed and the baryon mass is then realized by appropriately taking into account the center-of-mass correction, pionic correction, and gluonic correction. The EoS with the inclusion of hyperon-hyperon interaction mediated through the σ^* and ϕ mesons in three different coupling frameworks is developed in Sec. III. In Sec. IV we briefly describe the formalism to determine the tidal deformability and the moment of inertia of neutron stars. The results and discussions are made in Sec. V. We summarize our findings in Sec. VI.

II. MODIFIED QUARK-MESON COUPLING MODEL

The modified quark-meson coupling model has been broadly applied for the study of the bulk properties of symmetric and asymmetric nuclear matter. In an earlier work [14] this model was used to study the role of hyperons in neutron stars without taking in to consideration the contribution of the hyperon-hyperon interactions. We now extend this model to study the effect of strangeness in dense nuclear matter by including the contribution of the hidden strange mesons σ^* and ϕ. We begin by considering baryons as composed of three constituent quarks in a phenomenological flavor-independent confining potential, $U(r)$, in an equally mixed scalar and vector harmonic form inside the baryon [12], where

$$U(r) = \tfrac{1}{2}(1+\gamma^0)V(r),$$

with

$$V(r) = (ar^2 + V_0), \quad a > 0. \tag{1}$$

Here (a, V_0) are the potential parameters. The confining interaction provides the zeroth-order quark dynamics of the hadron. In the medium, the quark field $\psi_q(\mathbf{r})$ satisfies the Dirac equation

$$\big[\gamma^0\big(\epsilon_q - V_\omega - \tfrac{1}{2}\tau_{3q}V_\rho - V_\phi\big) - \vec{\gamma}\cdot\vec{p} - (m_q - V_\sigma - V_{\sigma^*}) - U(r)\big]\psi_q(\vec{r}) = 0, \tag{2}$$

where $V_\sigma = g^q_\sigma\sigma_0$, $V_\omega = g^q_\omega\omega_0$, $V_\rho = g^q_\rho b_{03}$, $V_\phi = g^q_\phi\phi_0$, and $V_{\sigma^*} = g^q_{\sigma^*}\sigma^*_0$. Here σ_0, ω_0, b_{03}, σ^*_0, and ϕ_0 are the classical meson fields, and g^q_σ, g^q_ω, g^q_ρ, $g^q_{\sigma_*}$, and g^q_ϕ are the quark couplings to the σ, ω, ρ, σ^*, and ϕ mesons respectively. m_q is the quark mass and τ_{3q} is the third component of the Pauli matrices. We can now define

$$\epsilon'_q = (\epsilon^*_q - V_0/2) \quad \text{and} \quad m'_q = (m^*_q + V_0/2), \tag{3}$$

where the effective quark energy, $\epsilon^*_q = \epsilon_q - V_\omega - \frac{1}{2}\tau_{3q}V_\rho - V_\phi$, and effective quark mass, $m^*_q = m_q - V_\sigma - V_{\sigma^*}$. We now introduce λ_q and r_{0q} as

$$(\epsilon'_q + m'_q) = \lambda_q \quad \text{and} \quad r_{0q} = (a\lambda_q)^{-\frac{1}{4}}. \tag{4}$$

The ground-state quark energy can be obtained from the eigenvalue condition

$$(\epsilon'_q - m'_q)\sqrt{\frac{\lambda_q}{a}} = 3. \tag{5}$$

The solution of Eq. (5) for the quark energy ϵ^*_q immediately leads to the mass of baryon in the medium in zeroth order as

$$E^{*0}_B = \sum_q \epsilon^*_q. \tag{6}$$

Corrections due to spurious center-of-mass motion, $\epsilon_{\text{c.m.}}$, as well as those due to other residual interactions, such as the one-gluon exchange at short distances, $(\Delta E_B)_g$, and quark-pion coupling arising out of chiral symmetry restoration, δM^π_B, have been considered in a perturbative manner, described explicitly in Refs. [12,14], to obtain the effective baryon mass.

Treating these energy corrections independently, the effective mass of the baryon in the medium becomes

$$M^*_B(\sigma,\sigma^*) = E^{*0}_B - \epsilon_{\text{c.m.}} + \delta M^\pi_B + (\Delta E_B)^E_g + (\Delta E_B)^M_g. \tag{7}$$

III. THE EQUATION OF STATE

To describe the properties of the core of a neutron star, we extend the usual Lagrangian density in the relativistic mean field approximation to include not only the σ, ω, and ρ mesons but also the strange mesons, namely the isoscalar, scalar (σ^*), and vector (ϕ) mesons. The Lagrangian density is, thus, chosen to be

$$\begin{aligned}\mathcal{L} = &\sum_B \bar{\psi}_B[i\gamma^\mu\partial_\mu - M^*_B(\sigma,\sigma^*) - g_{\omega B}\gamma^\mu\omega_\mu \\ &- g_{\phi B}\gamma^\mu\phi_\mu - g_{\rho B}\gamma^\mu\vec{\rho}_\mu\cdot\vec{I}_B]\psi_B \\ &+ \frac{1}{2}\big(\partial_\mu\sigma\,\partial^\mu\sigma - m^2_\sigma\sigma^2\big) + \frac{1}{2}\big(\partial_\mu\sigma^*\partial^\mu\sigma^* - m^2_{\sigma^*}\sigma^{*2}\big) \\ &+ \frac{1}{2}m^2_\omega\omega_\mu\omega^\mu - \frac{1}{4}\Omega_{\mu\nu}\Omega^{\mu\nu} + \frac{1}{2}m^2_\phi\phi_\mu\phi^\mu - \frac{1}{4}\Phi_{\mu\nu}\Phi^{\mu\nu} \\ &+ \frac{1}{2}m^2_\rho\vec{b}_\mu\cdot\vec{b}^\mu - \frac{1}{4}\vec{B}_{\mu\nu}\cdot\vec{B}^{\mu\nu} + \Lambda_v g^2_\omega g^2_\rho(\omega_\mu\omega^\mu)(\vec{b}_\mu\cdot\vec{b}^\mu) \\ &+ \sum_l \bar{\psi}_l[i\gamma^\mu\partial_\mu - m_l]\psi_l, \end{aligned} \tag{8}$$

where

$$\begin{aligned}\Omega_{\mu\nu} &= \partial_\mu\omega_\nu - \partial_\nu\omega_\mu, \\ \Phi_{\mu\nu} &= \partial_\mu\phi_\nu - \partial_\nu\phi_\mu, \\ \vec{B}_{\mu\nu} &= \partial_\mu\vec{b}_\nu - \partial_\nu\vec{b}_\mu, \end{aligned} \tag{9}$$

with $\psi_{B(l)}$ the baryon (lepton) field and $\vec{I}_B$ the isospin matrix for the baryon and m_l the lepton mass. The hadronic matter is described using a mean field approach in which the meson fields are treated as classical fields and the field operators are replaced by their expectation values. The meson field

equations in uniform matter are given by

$$m_\sigma^2\sigma_0 = \sum_B g_{\sigma B} C_B(\sigma)\rho_B^s, \tag{10}$$

$$m_{\sigma^*}^2\sigma_0^* = \sum_B g_{\sigma^* B} C_B(\sigma^*)\rho_B^s, \tag{11}$$

$$m_\omega^{*2}\omega_0 = \sum_B g_{\omega B}\rho_B, \tag{12}$$

$$m_\rho^{*2} b_{03} = \sum_B g_{\rho B} I_{3B}\rho_B, \tag{13}$$

$$m_\phi^2\phi_0 = \sum_B g_{\phi B}\rho_B, \tag{14}$$

where

$$\begin{aligned} m_\omega^{*2} &= m_\omega^2 + 2\Lambda_v g_\rho^2 g_\omega^2 b_{03}^2, \\ m_\rho^{*2} &= m_\rho^2 + 2\Lambda_v g_\rho^2 g_\omega^2 \omega_0^2. \end{aligned} \tag{15}$$

Here, I_{3B} is the isospin projection and Λ_v is a nonlinear ω-ρ coupling term [23] which gives rise to effective masses for the ω and ρ mesons. The scalar density, ρ_B^s, and the baryon density, ρ_B, are given as

$$\rho_B^s = \frac{\gamma}{2\pi^2}\int_0^{k_B} \frac{M_B^*}{\sqrt{k^2 + M_B^{*2}}} k^2 dk, \tag{16}$$

$$\rho_B = \frac{\gamma}{2\pi^2}\int_0^{k_B} k^2 dk = \frac{\gamma}{6\pi^2} k_B^3, \tag{17}$$

where $\gamma = 2$ is the spin degeneracy. In the above equations k_B is the Fermi momentum of the baryon species B ($B = N,\ \Lambda,\ \Sigma^{\pm},\ \Sigma^0,\ \Xi^-,\ \Xi^0$) respectively and $g_{\sigma B}C_B(\sigma)$ and $g_{\sigma^* B}C_B(\sigma^*)$ are given as

$$\begin{aligned} g_{\sigma B}C_B(\sigma) &= -\frac{\partial M_B^*(\sigma,\sigma^*)}{\partial\sigma}, \\ g_{\sigma^* B}C_B(\sigma^*) &= -\frac{\partial M_B^*(\sigma,\sigma^*)}{\partial\sigma^*}. \end{aligned} \tag{18}$$

The total energy density (ε) and pressure (p) at a particular baryon density for the nuclear matter in β equilibrium, consisting of the baryon octet and the leptons $l = e, \mu$ can be found as

$$\begin{aligned} \varepsilon = {} & \frac{1}{2}m_\sigma^2\sigma_0^2 + \frac{1}{2}m_{\sigma^*}^2\sigma_0^{*2} + \frac{1}{2}m_\omega^2\omega_0^2 + \frac{1}{2}m_\phi^2\phi_0^2 \\ & + \frac{1}{2}m_\rho^2 b_{03}^2 + \frac{\gamma}{2\pi^2}\sum_B\int_0^{k_B} k^2 dk\sqrt{k^2 + M_B^{*2}} \\ & + 3g_\omega^2 g_\rho^2\Lambda_v b_{03}^2\omega_0^2 + \sum_l \frac{1}{\pi^2}\int_0^{k_l} k^2 dk\sqrt{k^2 + m_l^2}, \end{aligned} \tag{19}$$

$$\begin{aligned} p = {} & -\frac{1}{2}m_\sigma^2\sigma_0^2 - \frac{1}{2}m_{\sigma^*}^2\sigma_0^{*2} + \frac{1}{2}m_\omega^2\omega_0^2 \\ & + \frac{1}{2}m_\phi^2\phi_0^2 + \frac{1}{2}m_\rho^2 b_{03}^2 + g_\omega^2 g_\rho^2\Lambda_v b_{03}^2\omega_0^2 \\ & + \frac{\gamma}{6\pi^2}\sum_B\int_0^{k_B} \frac{k^4\, dk}{\sqrt{k^2 + M_B^{*2}}} \\ & + \frac{1}{3}\sum_l \frac{1}{\pi^2}\int_0^{k_l} \frac{k^4 dk}{\left[k^2 + m_l^2\right]^{1/2}}. \end{aligned} \tag{20}$$

The chemical potentials, necessary to define the β-equilibrium conditions, are given by

$$\mu_B = \sqrt{k_B^2 + M_B^{*2}} + g_\omega\omega_0 + g_\rho I_{3B} b_{03} + g_\phi\phi_0. \tag{21}$$

The positive real solutions of $(k_e^2 + m_e^2)^{1/2} = \mu_e$ and $(k_\mu^2 + m_\mu^2)^{1/2} = \mu_\mu$ give the lepton Fermi momenta.

Since we consider the octet baryons, the presence of strange baryons in the matter plays a significant role. We define the strangeness fraction as

$$f_s = \frac{1}{3}\frac{\sum_i |s_i|\rho_i}{\rho}. \tag{22}$$

Here s_i refers to the strangeness number of baryon i and ρ_i is defined as $\rho_i = \gamma k_{Bi}^3/(6\pi^2)$.

The composition of neutron star matter with strongly interacting baryons is determined by the requirements of charge neutrality and β-equilibrium conditions under the weak processes. The charge neutrality condition after deleptonization is given by

$$q_{\rm tot} = \sum_B q_B\frac{\gamma k_B^3}{6\pi^2} + \sum_{l=e,\mu} q_l\frac{k_l^3}{3\pi^2} = 0, \tag{23}$$

where q_B corresponds to the electric charge of baryon species B and q_l corresponds to the electric charge of lepton species l in a star. The equilibrium composition of the star is obtained by solving Eqs. (10) to (11) in conjunction with the charge neutrality condition, given in Eq. (23), at a given total baryonic density $\rho = \sum_B \rho_B$. The effective masses of the baryons are obtained self-consistently in this model.

The net strangeness is determined by the condition of β equilibrium which for baryon B is given by $\mu_B = b_B\mu_n - q_B\mu_e$, where μ_B is the chemical potential of baryon B and b_B its baryon number, and q_B is the charge of the baryon under consideration. Thus the chemical potential of any baryon can be obtained [24] from the two independent chemical potentials μ_n and μ_e of neutron and electron respectively.

A. Baryon-meson coupling constants

The Baryon-Meson coupling constants are given by

$$g_{\omega B} = x_{\omega B} g_{\omega N}, \quad g_{\rho B} = x_{\rho B} g_{\rho N},$$

where $x_{\omega B}$ and $x_{\rho B}$ are equal to 1 for the nucleons and acquire different values in different parametrizations for the other baryons. We note that the s quark is unaffected by the σ and ω mesons, i.e., $g_\sigma^s = g_\omega^s = 0$. To take into account the effect of the strange quark, we include the strange mesons σ^* and ϕ with couplings g_{σ^*} and g_ϕ respectively. The isoscalar-scalar and isoscalar-vector couplings g_σ^q and g_ω are fitted to the saturation density and binding energy for nuclear matter. The

isovector vector coupling to the nucleon g_ρ is set by fixing the symmetry energy at $J = 32.0$ MeV.

The vector-meson couplings to the hyperons are fixed using three different approaches to get three parameter sets, Set I, Set II, and Set III. In the first set we use the SU(6) spin-flavor symmetry [25,26] as follows:

$$\begin{aligned} \frac{1}{3}g_{\omega N} &= \frac{1}{2}g_{\omega\Lambda} = \frac{1}{2}g_{\omega\Sigma} = g_{\omega\Xi}, \\ g_{\rho N} &= g_{\rho\Lambda} = \frac{1}{2}g_{\rho\Sigma} = g_{\rho\Xi}, \\ 2g_{\phi\Lambda} &= 2g_{\phi\Sigma} = g_{\phi\Xi} = -\frac{2\sqrt{2}}{3}g_{\omega N}, \end{aligned} \tag{24}$$

with $g_{\phi N} = 0$.

In Set II, we adjust the ω-hyperon coupling strengths ($x_{\omega\Lambda}$, $x_{\omega\Sigma}$, and $x_{\omega\Xi}$) to the hyperon-nucleon interaction potential at saturation density for the Λ, Σ, and Ξ hyperons with $U_\Lambda = -28$ MeV, $U_\Sigma = 30$ MeV, and $U_\Xi = -18$ MeV respectively [22,27] using the relation $U_B = -(M_B - M_B^*) + x_{\omega B} g_\omega \omega_0$ for $B = \Lambda$, Σ, and Ξ. The ϕ-baryon coupling is kept the same as that in Set I and the ρ coupling to the hyperons is fixed to be the same as that of the nucleons.

For Set III, we use the more general SU(3) flavor symmetry. The SU(3) group with three flavors of quarks (up, down, strange) is regarded as the symmetry group for strong interactions. We follow the scheme given in Refs. [22,28–31] using the matrix representations for the baryon octet and meson nonet (singlet state and octet state). In such a scheme, the ω and ϕ mesons are described in terms of the pure singlet, $|1\rangle$, and octet, $|8\rangle$, states as

$$\begin{aligned} \omega &= \cos\theta_v|1\rangle + \sin\theta_v|8\rangle \\ \phi &= -\sin\theta_v|1\rangle + \cos\theta_v|8\rangle, \end{aligned} \tag{25}$$

with θ_v being the mixing angle. The mixing angle is fixed using the Nijmegen extended-soft-core (ESC) model [28]. The values of the θ_v and z ($z \equiv g_8/g_1$, coupling ratio of the octet to singlet coupling constants), suggested in the ESC model are given as

$$\theta_v = 37.50^\circ, \quad z = 0.1949. \tag{26}$$

Then the relations of the vector-meson–hyperon coupling constants in SU(3) are defined as

$$\begin{aligned} g_{\omega\Lambda} &= g_{\omega\Sigma} = \frac{1}{1+\sqrt{3}z\tan\theta_v}g_{\omega N}, \\ g_{\omega\Xi} &= \frac{1-\sqrt{3}z\tan\theta_v}{1+\sqrt{3}z\tan\theta_v}g_{\omega N} \end{aligned} \tag{27}$$

$$\begin{aligned} g_{\phi N} &= \frac{\sqrt{3}z-\tan\theta_v}{1+\sqrt{3}z\tan\theta_v}g_{\omega N}, \\ g_{\phi\Lambda} &= g_{\phi\Sigma} = \frac{-\tan\theta_v}{1+\sqrt{3}z\tan\theta_v}g_{\omega N}, \\ g_{\phi\Xi} &= -\frac{\sqrt{3}z+\tan\theta_v}{1+\sqrt{3}z\tan\theta_v}g_{\omega N}. \end{aligned} \tag{28}$$

In all the three sets considered above we have fixed $g_\sigma^* = 2$ considering a weak hyperon-hyperon coupling. The meson mean fields σ_0, ω_0, b_{03}, ϕ_0, and σ_0^* are determined through self-consistently using the field equations (10)–(14).

The relation between the mass and radius of a star with its central density can be determined by integrating the Tolman-Oppenheimer-Volkoff (TOV) equations [32–34] given by

$$\frac{dp}{dr} = -\frac{G(mc^2 + 4\pi r^3 p)(\varepsilon + p)}{rc^4(r - 2Gm/c^2)}, \tag{29}$$

$$\frac{dm}{dr} = 4\pi r^2 \frac{\varepsilon}{c^2}, \tag{30}$$

with G as the gravitational constant, c is the speed of light, and m representing the mass interior to the radius r. Using the EoS obtained from the three different parameter sets and integrating the TOV equations from the origin as an initial value problem for a given choice of the central energy density, ε_0, we determine the maximum mass of a star. The surface of the star is defined from the value of $r(=R)$, where the pressure vanishes. It may be noted here that we have used the standard Baym-Pethick-Sutherland (BPS) EoS [35] for the low density.

IV. NEUTRON STAR TIDAL DEFORMABILITY AND MOMENT OF INERTIA

The in-spiral phase of two merging neutron stars creates strong tidal gravitational fields resulting in the deformation of the multipolar structure of the star. Such deforming effects are quantified through the tidal deformability parameter λ, which relates the induced mass quadruple moment Q_{ij} to the time-independent external tidal field $\mathcal{E}_{ij}$ through the relation

$$Q_{ij} = -\lambda \mathcal{E}_{ij}. \tag{31}$$

For a static spherically symmetric star of mass M and radius R, the tidal deformation parameter λ can be expressed in terms of the dimensionless Love number k_2 (for the leading order $l = 2$) as

$$\lambda = \tfrac{2}{3}k_2 R^5. \tag{32}$$

The tidal Love number k_2 is given by [36–38],

$$\begin{aligned} k_2 = {} & \tfrac{8}{5}\beta^5(1-2\beta)^2[2 - y_R + 2\beta(y_R - 1)] \\ & \times \{2\beta[6 - 3y_R + 3\beta(5y_R - 8)] \\ & + 4\beta^3[13 - 11y_R + \beta(3y_R - 2) \\ & + 2\beta^2(1 + y_R)] + 3(1-2\beta)^2[2 - y_R \\ & + 2\beta(y_R - 1)]\ln(1-2\beta)\}^{-1}, \end{aligned} \tag{33}$$

where $\beta \equiv GM/Rc^2$ is the dimensionless compactness parameter. The quantity $y_R \equiv y(R)$ satisfies the first-order differential equation

$$\frac{dy}{dr} = -\frac{y^2}{r} - \frac{y-6}{r - 2Gm/c^2} - rQ, \tag{34}$$

with

$$\begin{aligned} Q = {} & \frac{4\pi G}{c^4}\frac{(5-y)\varepsilon + (9+y)p + (\varepsilon + p)/c_s^2}{1 - 2Gm/c^2} \\ & - \left[\frac{2G(m + 4\pi pr^3/c^2)}{r(rc^2 - 2Gm)}\right]^2, \end{aligned} \tag{35}$$

TABLE I. The potential parameter V_0 for different baryons obtained for the quark mass $m_u = m_d = 200$ MeV, $m_s = 300$ MeV, with $a = 0.722\,970\,\text{fm}^{-3}$.

Baryon	M_B (MeV)	V_0 (MeV)
N	939	5.44
Λ	1115.6	28.00
Σ	1193.1	43.29
Ξ	1321.3	54.17

where $c_s^2 = d\varepsilon/dp$ is the squared speed of sound. Equation (34) needs to be integrated self-consistently along with the TOV equations (30) with the boundary conditions at $r = 0$ such that $y(0) = 2$, $m(0) = 0$, and $p(0) = p_c$.

Since the accumulation of phase difference of the gravitational waves determines the tidal deformability, a dimensionless deformability parameter Λ_D appearing in the dimensionless phase may be defined as [1,36,39],

$$\Lambda_D = \frac{2}{3}\frac{k_2}{\beta^5}. \tag{36}$$

For a binary system comprising of two component stars having masses M_1 and M_2 ($M_1 \geqslant M_2$) with mass ratio $q = M_2/M_1$, the chirp mass is given by

$$\mathcal{M} = \frac{(M_1 M_2)^{3/5}}{(M_1 + M_2)^{1/5}}. \tag{37}$$

For such a system the mass weighted average dimensionless tidal deformability $\widetilde{\Lambda}$ is defined as

$$\widetilde{\Lambda} = \frac{16}{13}\frac{(M_1 + 12M_2)M_1^4\Lambda_1 + (M_2 + 12M_1)M_2^4\Lambda_2}{(M_1 + M_2)^5}, \tag{38}$$

where Λ_1 and Λ_2 are the tidal deformabilities of the component masses M_1 and M_2 respectively.

For a uniformly slowly rotating star the moment of inertia can be determined using

$$I = \frac{w_R R^3}{6 + 2w_R}, \tag{39}$$

where w_R is the solution, at the surface R, of the differential equation

$$\frac{dw}{dr} = \frac{4\pi G}{c^2}\frac{r(\varepsilon + p)(4 + w)}{c^2 - 2Gm} - \frac{w(3 + w)}{r} \tag{40}$$

with the condition $w(0) = 0$.

TABLE II. The quark meson couplings g_σ^q, g_ω, and g_ρ for nuclear matter at quark mass $m_q = 200$ MeV. g_ρ is determined keeping nonlinear coupling fixed at $\Lambda_v = 0.05$. Also shown are the values of the nucleon effective mass and the nuclear matter incompressibility K.

m_q (MeV)	g_σ^q	g_ω	g_ρ	M_N^*/M_N	K (MeV)
200	4.36839	7.40592	9.39956	0.83	242.41

TABLE III. $x_{\omega B}$ determined for parameter Set II by fixing the potentials for the hyperons.

m_q (MeV)	$x_{\omega\Lambda}$ $U_\Lambda = -28$ MeV	$x_{\omega\Sigma}$ $U_\Sigma = 30$ MeV	$x_{\omega\Xi}$ $U_\Xi = -18$ MeV
200	0.81316	1.43857	0.43399

V. RESULTS AND DISCUSSION

A. EoS and the mass-radius relations

In the following we first discuss the results of the inclusion of the strange interaction in the MQMC for the three different coupling sets. There are two potential parameters in the relativistic quark model, a and V_0 which are obtained by fitting the nucleon mass $M_N = 939$ MeV and charge radius of the proton $\langle r_N \rangle = 0.84$ fm in free space. Keeping the value of the potential parameter a same as that for nucleons, we obtain V_0 for the Λ, Σ, and Ξ baryons by fitting their respective masses to $M_\Lambda = 1115.6$ MeV, $M_\Sigma = 1193.1$ MeV and $M_\Xi = 1321.3$ MeV. The mass of the u, d quarks is fixed at 200 MeV and the mass of the s quark is fixed at 300 MeV, keeping in view the experimental constraints available for the nuclear matter incompressibility and the radius corresponding to a $1.4M_\odot$ ($R_{1.4}$) neutron star ($9.9 < R_{1.4} < 13.6$ km). The set of potential parameters for the baryons are given in Table I.

The incompressibility K of symmetric nuclear matter for quark mass 200 MeV comes out to be 242.41 MeV. Recent measurements [40] extracted from doubly-magic nuclei like ^{208}Pb constrain the value of K to be around 240 ± 20. The quark meson couplings g_σ^q, $g_\omega = 3g_\omega^q$, and $g_\rho = g_\rho^q$ are fitted self-consistently for the nucleons to obtain the correct saturation properties of nuclear matter binding energy, $E_{B.E.} \equiv B_0 = \varepsilon/\rho_B - M_N = -15.7$ MeV, pressure, $p = 0$, and symmetry energy $J = 32.0$ MeV at saturation density, $\rho_0 = 0.15\,\text{fm}^{-3}$.

We have taken the standard values for the meson masses; namely, $m_\sigma = 550$ MeV, $m_\omega = 783$ MeV, $m_\rho = 763$ MeV, $m_{\sigma^*} = 980$ MeV, and $m_\phi = 1020$ MeV. The values of the quark meson couplings, g_σ^q, g_ω, and g_ρ at quark masses 200 MeV are given in Table II. The value of the ω-ρ coupling term Λ_v, which affects the g_ρ coupling [14], is fixed at $\Lambda_v = 0.05$. In fact, such a nonlinear ω-ρ term gives rise to effective masses for the ω and ρ mesons, thus softening the vector fields at large densities [41], as given in Eq. (12).

As discussed in the previous section, we use three types of parameter sets for the nonstrange and strange meson couplings to the hyperons. For Set I we use the SU(6) spin-flavor

TABLE IV. Effect of variation of $g_{\sigma*}$ on the $U_\Lambda^{(\Lambda)}$ and mass-radius relation.

$g_{\sigma*}$	M ($M_\odot$)	R (km)	$U_\Lambda^{(\Lambda)}(\rho_0/5)$
4	1.88	11.3	−3.88
3	1.89	11.3	−3.88
2	1.90	11.2	−3.88
1	1.90	11.2	−3.93

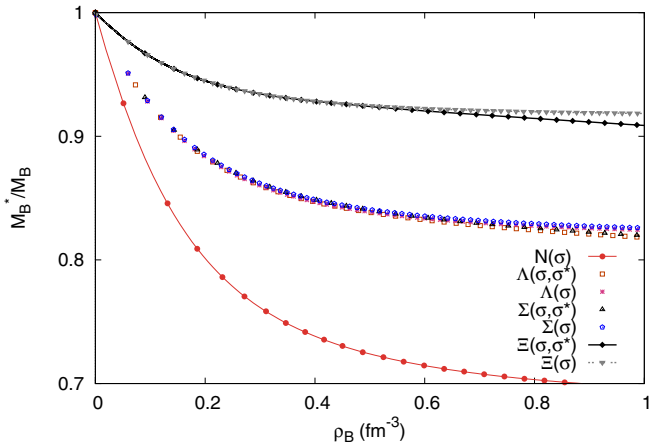

FIG. 1. Effective mass of baryons as a function of baryon density. The interactions involving only σ is shown with $B(\sigma)$ while those with both (σ, σ^*) are shown as $B(\sigma, \sigma^*)$.

symmetry. For Set II we follow a mixed scheme where the hyperon couplings to the ω meson are fixed by determining $x_{\omega B}$. The value of $x_{\omega B}$ is obtained from the hyperon potentials

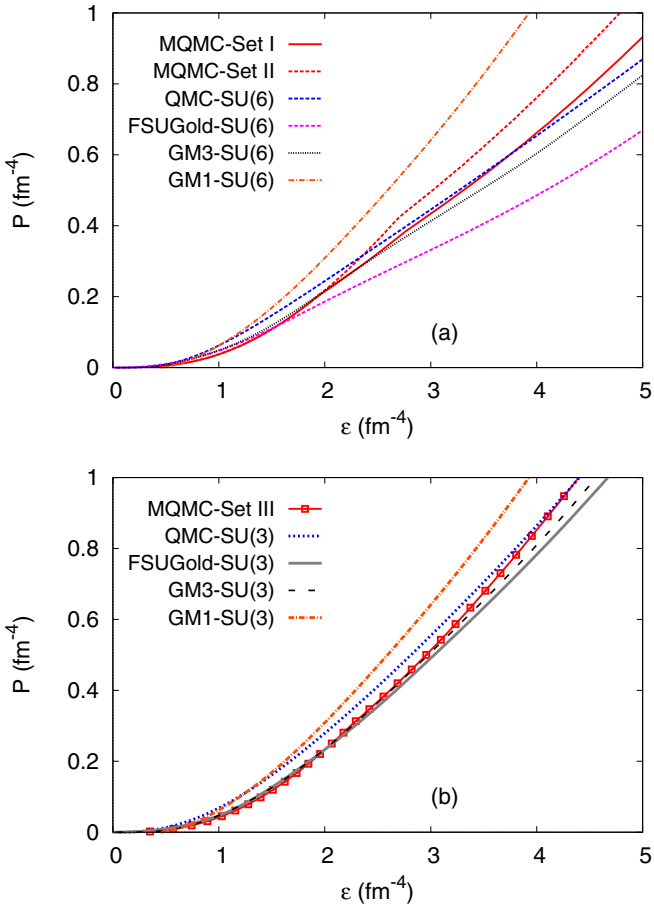

FIG. 2. Total pressure as a function of the energy density at quark mass $m_q = 200$ MeV. Panel (a) shows Set I and Set II of the MQMC model as compared to the QMC, FSUGold, and GM3 parametrizations in SU(6) while (b) shows the comparison of Set III EoS of the MQMC model with QMC, FSUGold, and GM3 parametrizations in SU(3).

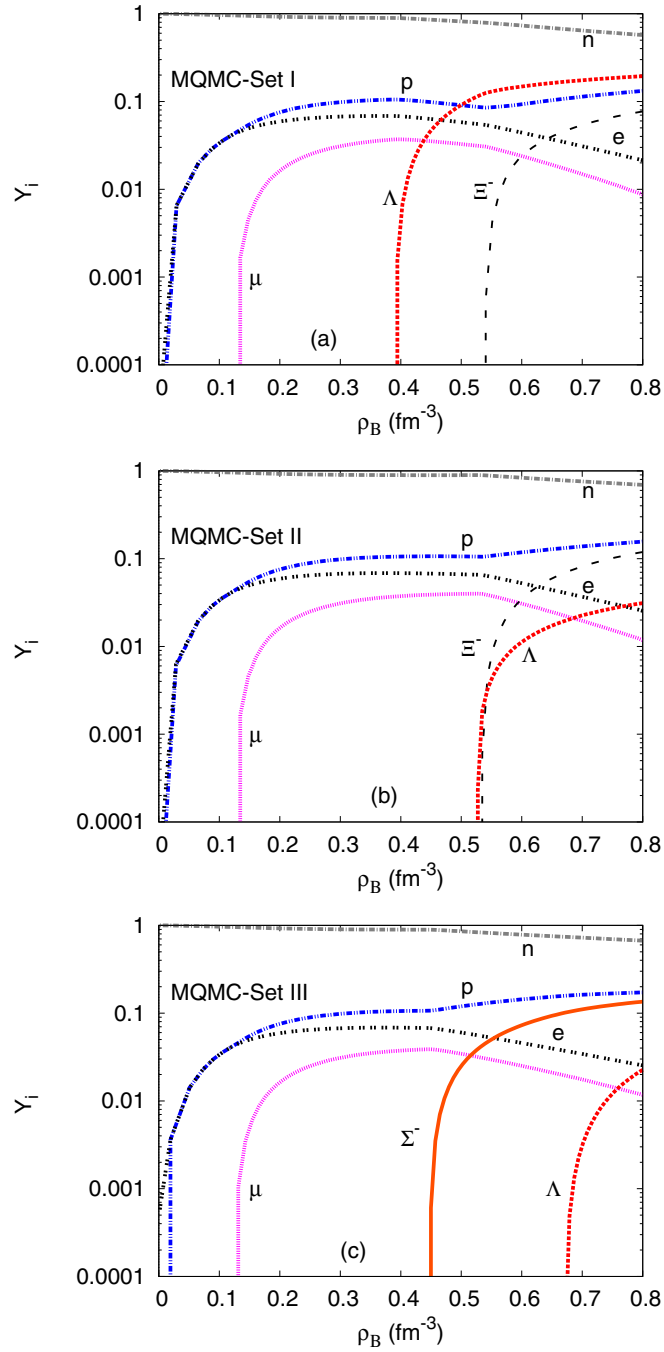

FIG. 3. Particle fraction for the three parameter sets.

in nuclear matter, $U_B = -(M_B - M_B^*) + x_{\omega B} g_\omega \omega_0$ for $B = \Lambda$, Σ, and Ξ as -28, 30, and -18 MeV respectively. For the quark mass 200 MeV the corresponding values for $x_{\omega B}$ are given in Table III. The value of $x_{\rho B} = 1$ is fixed for all baryons in this parameter set. For Set III we use the SU(3) flavor symmetry to fix the couplings of the ω and ϕ mesons with the hyperons. As indicated from the Nagara event [42], which suggests the depth of the potential between two Λ's is about -5 MeV, we choose the coupling of the strange meson σ^* to be weak at 2.0. In fact, using parameter Set III we determine

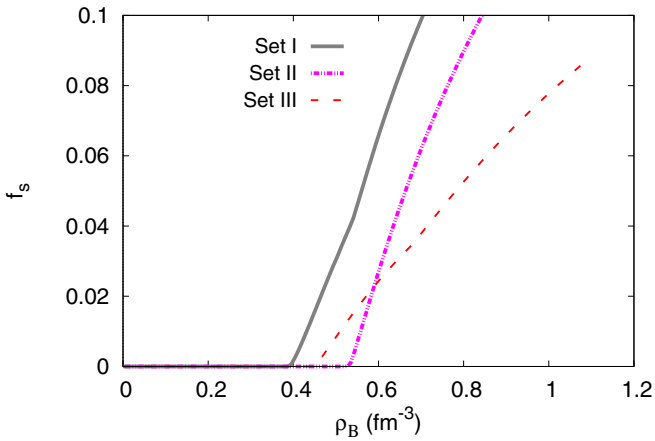

FIG. 4. Strangeness fraction as a function of density for Sets I, II, and III.

the value of the potential $U_\Lambda^{(\Lambda)}$ for Λ in Λ-hyperon matter as

$$U_\Lambda^{(\Lambda)} = -g_{\sigma\Lambda}\sigma_0^{(\Lambda)} - g_{\sigma^*\Lambda}\sigma_0^{*(\Lambda)} + g_{\omega\Lambda}\omega_0^{(\Lambda)} + g_{\phi\Lambda}\phi_0^{(\Lambda)}, \tag{41}$$

which comes out as -5.28 MeV at saturation density ρ_0. Recent studies on hypernuclear matter [43–45] provide a range of -14 to $+9$ MeV for $U_\Lambda^{(\Lambda)}(\rho_0)$ implying thereby a range for $U_\Lambda^{(\Lambda)}(\rho_0/5)$ between -5 and -11 MeV [44]. Hence our value $U_\Lambda^{(\Lambda)}$ as well as $U_\Lambda^{(\Lambda)}(\rho_0/5) = -3.88$ MeV lie within the expected range according to [43–45]. Again we further notice that the effect of minor variation of the strength of $g_{\sigma*}$ does not significantly change the value of $U_\Lambda^{(\Lambda)}(\rho_0/5)$, as can be seen in the Table IV.

Figure 1 shows the effective baryon mass, M_B^*/M_B, as a function of baryon density. At saturation density ρ_0 the value of M_B^*/M_B is 0.83 for nucleons. The effect of the inclusion of strange meson σ^* on the baryon mass can be observed in the figure. The dotted lines indicate the variation in baryon mass in the absence of the σ^* meson while the continuous lines show the variation with the inclusion of σ^*. The additional strange interaction affects only the hyperons as σ^* interacts only with strange baryons and decreases the effective mass of the hyperons.

TABLE V. Mass and radius for different parameter sets of MQMC and other considered RMF models using SU(3) symmetry. Also shown is the radius corresponding to the canonical mass $1.4M_\odot$.

Set	M ($M_\odot$)	R (km)	$R_{1.4}$ (km)
MQMC-Set I	1.66	11.2	12.7
MQMC-Set II	1.79	11.3	12.7
MQMC-Set III	1.90	11.2	13.1
QMC-SU(3)	1.93	11.8	13.6
FSUGold-SU(3)	1.79	11.2	12.8
GM3-SU(3)	1.85	11.4	13.3
GM1-SU(3)	2.14	12.2	13.9

The EoS for the different parameter sets I, II, and III in the MQMC model is shown in Figs. 2(a) and 2(b) and also compared with the results [22] from QMC [46], FSUGold [47], GM1, and GM3 [8] calculations. Recently various studies [48–50] have comprehensively analysed a wide set of relativistic mean field (RMF) models with nucleonic and hyperonic composition to study stellar properties. The results for the present work are compared with the extended version [22] of the QMC, FSUGold, GM1, and GM3 models which consider iso-scalar, vector-meson couplings to the octet baryons in both SU(3) and SU(6) symmetry. Out of these only FSUGold uses a nonlinear ω-ρ coupling term $\Lambda_v = 0.03$ while QMC, GM1, and GM3 do not use such an interaction. It is observed that parameter Set II gives the stiffest EoS when compared to other SU(6) models. We also observe that EoS from SU(3) sets are comparatively more stiff than those from SU(6). This occurs due to the enhanced vector-meson couplings to the baryons in SU(3) symmetry.

Figure 3 shows the particle fractions for the three types of parameter sets in β-equilibrated matter. Hyperons appear in all the sets chosen, though their threshold density of production differs with different meson-hyperon coupling sets. Σ^-

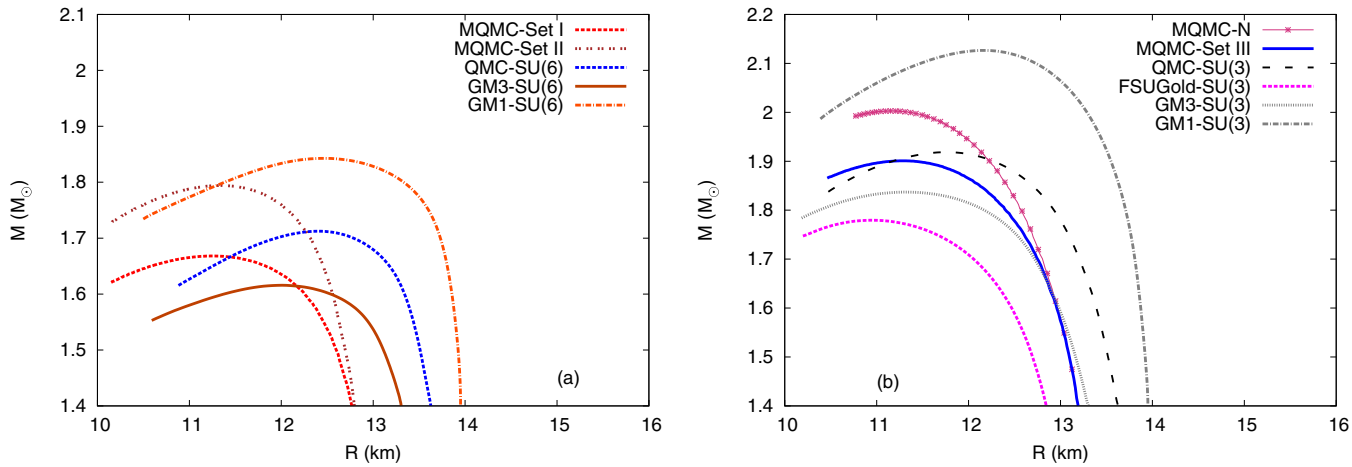

FIG. 5. Star mass as a function of radius for (a) Sets I and II and (b) Set III at $m_q = 200$ MeV along with the plots for the QMC, FSUGold, GM1, and GM3 models.

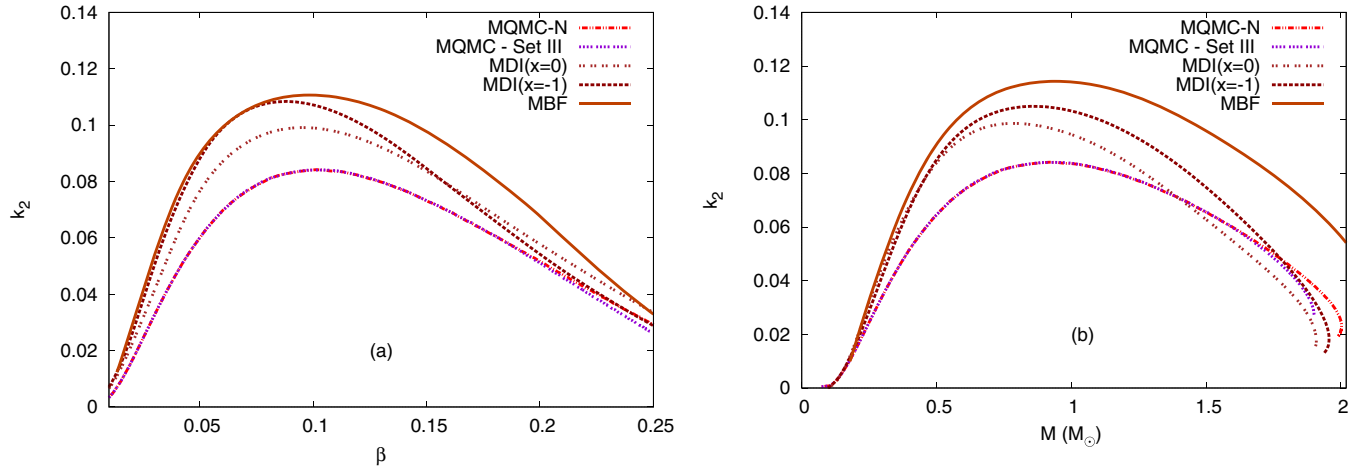

FIG. 6. Love number as a function of (a) compactness β and (b) mass of star for Set III and matter with only nucleons, represented by MQMC-N.

production is preferred in SU(3) coupling Set III, indicating suppression of Ξ fields at higher densities. Parameter Set II fixes a repulsive Σ-hyperon potential resulting in the absence of the Σ hyperon in the matter distribution.

Figure 4 shows the strangeness fraction for the three types of sets considered in the present model. It is observed that the strangeness fraction increases at lower densities for Set I with complete SU(6) couplings. Between Sets II and III, though the strangeness appears earlier in Set III, there is sharper increase in the fraction for Set II, indicating more strangeness content at lower densities. This is reflected in the EoS plot where the EoS for Set II is softer than that for Set III.

In Fig. 5 we plot the mass-radius relations for the different parameter sets. It is clearly observed that SU(6) sets fail to achieve the maximum mass limit of the pulsar PSR J1614-2230. Matter composed only of nucleons (MQMC-N) with no strange matter gives the highest mass of $2.0M_\odot$. However, with the inclusion of strange interactions, Set III employing the SU(3) coupling scheme is able to achieve a maximum mass of $1.90M_\odot$ with a corresponding radius of 11.2 km. The radius corresponding to the canonical $1.4M_\odot$ star for Set III is 13.1 km. For Sets I and II, the maximum mass is much lower, but the canonical radius is 12.7 km. The mass and radius for all the three sets as well as of the models QMC, FSUGold, GM1, and GM3 are shown in Table V. It is observed that GM1 provides the most massive star as compared to the other relativistic mean field models. However, its $R_{1.4}$ value exceeds the range $9.9 < R_{1.4} < 13.6$ km suggested from the recent GW170817 event.

B. Tidal deformability and the I-Love universal relation

The recent detection of event GW170817 [1] and the consequent studies involving radius measurements constrain the radii of $1.4M_\odot$ mass neutron stars, between $9.9 < R_{1.4} < 13.6$ km. In the present work we obtain $R_{1.4}$ at 13.1 km which lies within the predicted range. Furthermore, we observe that in the present model the SU(3) set is favorable for a massive star of $1.90M_\odot$ even with the inclusion of hyperons and strange interactions. Since the tidal deformabilities are measurable macroscopic quantities from gravitational wave observations, the EoS obtained using Set III (MQMC-Set III) is used to determine the Love number k_2 and the tidal

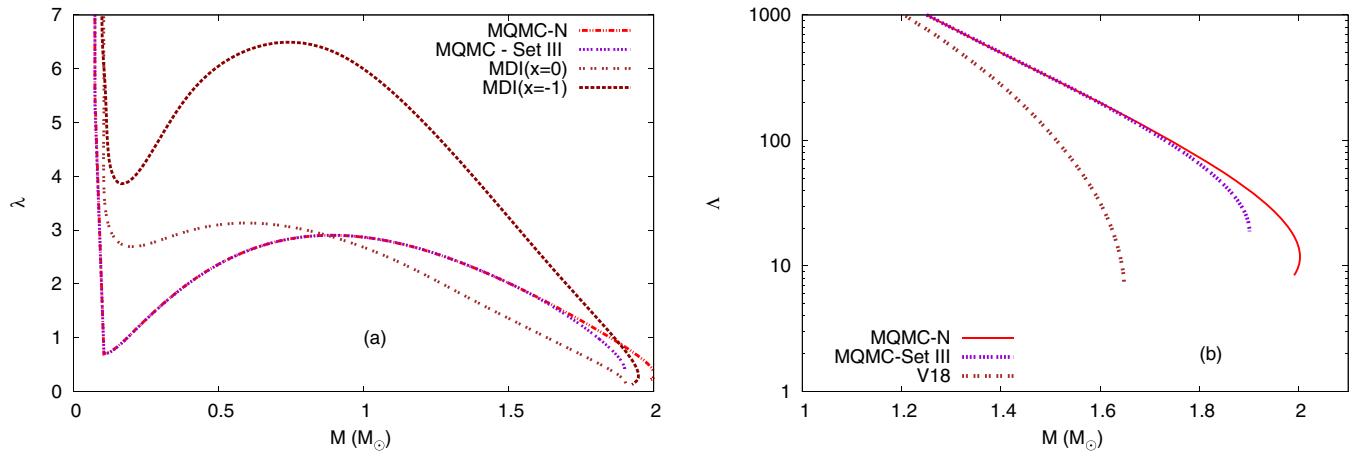

FIG. 7. (a) The tidal deformability parameter λ ($\times 10^{36}$ g cm^{2}s^2) and (b) the dimensionless tidal deformability Λ_D as a function of mass of star for Set III and MQMC-N.

TABLE VI. Mass, radius, and dimensionless tidal deformability Λ_D for MQMC EoS compared with another hyperonic and nucleonic EoS. Also shown is the radius corresponding to the canonical mass $1.4M_\odot$.

Set	M ($M_\odot$)	R (km)	$R_{1.4}$ (km)	$\Lambda_{D1.4}$
MQMC-N	2.00	11.1	13.1	484
MQMC-Set III	1.90	11.2	13.1	483
V18(N+Y)	1.65	9.0	11.9	302
DBHF	2.31	11.2	13.1	274

deformabilities λ and Λ_D as per the formalism given above. In Fig. 6(a) the Love number k_2 as a function of the compactness parameter β is shown for MQMC EoS composed only of the nucleons (MQMC-N) and the MQMC EoS obtained using Set III (MQMC-Set III). We compare these with the results from the many-body forces model involving strange interactions [51] and the momentum-dependent interaction (MDI) model [52] which uses a parameter x to account for the density dependence of nuclear symmetry energy. It is observed that the Love number decreases rapidly for higher values of β as well as for small values ($\beta < 0.1$). Figure 6(b) shows the variation of k_2 with stellar mass. It is observed that the value k_2 peaks near $1M_\odot$. For masses above and below the $1M_\odot$ range the k_2 value is lower due to less contribution of the tidal deformation on the quadrupole moment.

Figure 7(a) shows the tidal deformation parameter λ as a function of the stellar mass. It is observed that λ becomes larger for stars with a mass range of 0.5–1.0$M_\odot$. The dimensionless tidal deformability Λ_D as a function of the star mass is shown Fig. 7(b). We observe that Λ_D decreases as the neutron star mass increases. However, for a $1.4M_\odot$ star, the value of $\Lambda_D = 483$ satisfies the constraint of $\Lambda_D < 800$ obtained from GW170817. The values of M, R, $R_{1.4}$, and Λ_D for the MQMC EoS is compared with the V18 (N+Y) [53] and DBHF [54] EoS in Table VI.

Analysis of the GW170817 event also puts a constraint on the tidal effects in the in-spiral of two neutron stars through the mass weighted tidal deformability $\widetilde{\Lambda}$ determined using Eq. (38). Using the chirp mass $\mathcal{M} = 1.188^{+0.004}_{-0.002} M_\odot$ corresponding to a symmetric binary system with $M_1 = M_2 = 1.365M_\odot$, we obtain $\widetilde{\Lambda} = 624$, which lies within the limit $70 < \widetilde{\Lambda} < 720$ [7]. We calculate the neutron star moment of inertia using the MQMC-Set III and MQMC-N EoS considering slow rotation regimes using Eq. (39). In particular, we determine the dimensionless moment of inertia $\bar{I} = I/M^3$ which can be related to the dimensionless deformability Λ_D through EoS independent universal relations [55–57], referred to as the I-Love universal relations. The moment of inertia as a function of stellar mass is shown in Fig. 8(a). Since the neutron star radius remains nearly constant before reaching the maximum mass for a given EoS, the moment of inertia increases almost linearly with stellar mass. A sharp drop arises when the maximum mass is reached. In Fig. 8(b) we show the correlation between the dimensionless moment of inertia $\bar{I} = I/M^3$ and the dimensionless tidal deformability Λ_D and compare it with the universal fit [58] given by

$$\frac{I}{M^3} \equiv 0.8134\beta^{-1} + 0.2101\beta^{-2} + 0.003175\beta^{-3} - 0.0002717\beta^{-4}. \quad (42)$$

We observe very minute deviations of the MQMC EoS from the universal fit.

VI. CONCLUSION

In the present work we have developed the EoS using a relativistic quark model which considers the baryons to be composed of three independent relativistic quarks confined by an equal admixture of a scalar-vector harmonic potential in a background of scalar and vector mean fields. Appropriate corrections to the center-of-mass motion and to pionic and gluonic exchanges within the nucleon are calculated to obtain the effective mass of the baryon. The baryon-baryon interactions are realized by the quark coupling to the σ, ω, and ρ mesons through a mean field approximation. To include the

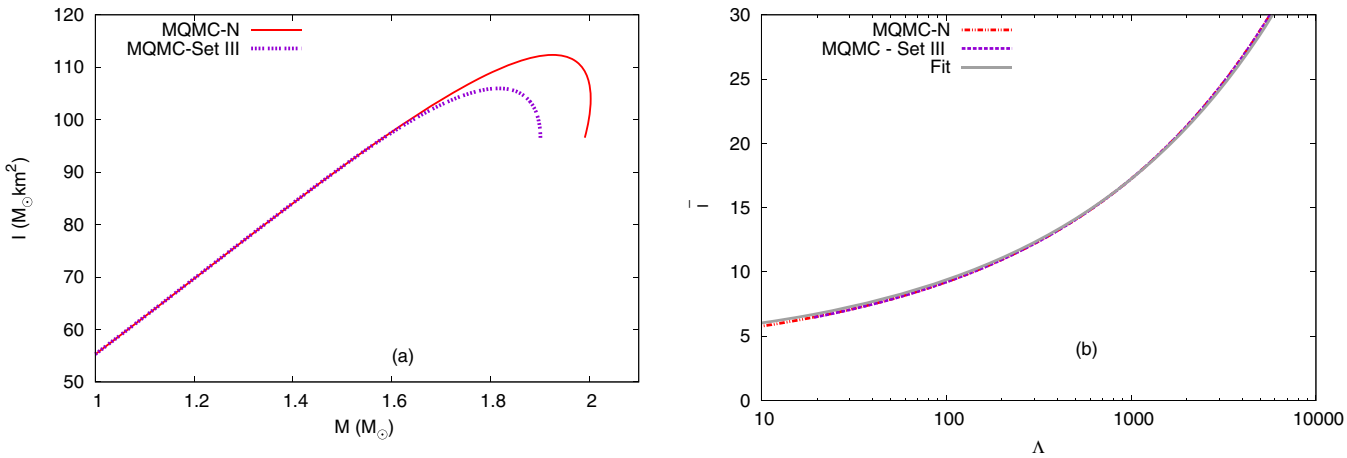

FIG. 8. (a) The moment of inertia as a function of the stellar mass. (b) The correlation between the dimensionless moment of inertia $\bar{I} = I/M^3$ and the dimensionless tidal deformability Λ_D compared with a fit given by Eq. (42).

contribution of strangeness, the hyperon-hyperon interaction mediated by σ^* and ϕ mesons is introduced.

The strange and nonstrange meson couplings to the hyperons are fixed using three different techniques based on symmetry considerations and the available hyperon-nucleon potentials. The EoS is analyzed for three different sets of coupling constants and the effect of such couplings on the strangeness fraction is studied. The variations of the maximum mass and radius in the present set of parametrizations are determined and it is observed that an extension of SU(6) spin-flavor symmetry to SU(3) flavor symmetry is favorable to obtain massive yet compact stars. Using the EoS obtained from the SU(3) set we determine the tidal love number k_2 and the tidal deformabilities λ and Λ_D. We further evaluate the weighted average tidal deformability $\widetilde{\Lambda}$ in a binary system of observed chirp mass $1.188M_\odot$. We find that the MQMC EoS with hyperonic matter and strange interactions satisfies all the recent constraints set by the GW170817 event. We further determine the moment of inertia of the neutron star and compare it with the available universal fits. We observe very minor deviations between the fits and our data.

ACKNOWLEDGMENTS

The authors would like to acknowledge financial assistance from BRNS, India, for Project No. 2013/37P/66/BRNS. H.S.S. would like to acknowledge support via CSIR-SRF Fellowship No. 09/1036/0007 (2018).

[1] B. P. Abbott *et al.* (LIGO Scientific Collaboration and Virgo Collaboration), Phys. Rev. Lett. **119**, 161101 (2017).
[2] E. Annala, T. Gorda, A. Kurkela, and A. Vuorinen, Phys. Rev. Lett. **120**, 172703 (2018).
[3] A. Bauswein, O. Just, H.-T. Janka, and N. Stergioulas, Astrophys. J. Lett. **850**, L34 (2017).
[4] B. Margalit and B. D. Metzger, Astrophys. J. Lett. **850**, L19 (2017).
[5] L. Rezzolla, E. R. Most, and L. R. Weih, Astrophys. J. Lett. **852**, L25 (2018).
[6] M. Ruiz, S. L. Shapiro, and A. Tsokaros, Phys. Rev. D **97**, 021501(R) (2018).
[7] B. P. Abbott *et al.*, Phys. Rev. X **9**, 011001 (2019).
[8] N. K. Glendenning and S. A. Moszkowski, Phys. Rev. Lett. **67**, 2414 (1991); M. Hanauske, D. Zschiesche, S. Pal, S. Schramm, and W. G. H. Stocker, Astrophys. J. **537**, 958 (2000); S. Schramm and D. Zschiesche, J. Phys. G **29**, 531 (2003); W. H. Long, B. Y. Sun, K. Hagino, and H. Sagawa, Phys. Rev. C **85**, 025806(R) (2012).
[9] R. Knorren, M. Prakash, and P. J. Ellis, Phys. Rev. C **52**, 3470 (1995).
[10] S. Balberg and A. Gal, Nucl. Phys. A **625**, 435 (1997).
[11] M. Prakash, I. Bombaci, M. Prakash, P. J. Ellis, and J. M. Lattimer, Phys. Rep. **280**, 1 (1997).
[12] N. Barik, R. N. Mishra, D. K. Mohanty, P. K. Panda, and T. Frederico, Phys. Rev. C **88**, 015206 (2013).
[13] R. N. Mishra, H. S. Sahoo, P. K. Panda, N. Barik, and T. Frederico, Phys. Rev. C **92**, 045203 (2015).
[14] R. N. Mishra, H. S. Sahoo, P. K. Panda, N. Barik, and T. Frederico, Phys. Rev. C **94**, 035805 (2016).
[15] H. S. Sahoo, G. Mitra, R. N. Mishra, P. K. Panda, and B. A. Li, Phys. Rev. C **98**, 045801 (2018).
[16] N. Barik and B. K. Dash, Phys. Rev. D **33**, 1925 (1986); **34**, 2092(E) (1986).
[17] N. Barik and R. N. Mishra, Phys. Rev. D **61**, 014002 (1999).
[18] X. Xing, J. Hu, and H. Shen, Phys. Rev. C **95**, 054310 (2017).
[19] Z.-Y. Zhu, E.-P. Zhou, and A. Li, Astrophys. J. **862**, 98 (2018).
[20] J. Beringer *et al.* (Particle Data Group), Phys. Rev. D **86**, 010001 (2012).
[21] A. Pais, Rev. Mod. Phys. **38**, 215 (1966).
[22] T. Miyatsu, M. K. Cheoun, and K. Saito, Phys. Rev. C **88**, 015802 (2013).
[23] C. J. Horowitz and J. Piekarewicz, Phys. Rev. Lett. **86**, 5647 (2001).
[24] P. K. Panda, D. P. Menezes, and C. Providencîa, Phys. Rev. C **69**, 025207 (2004).
[25] C. Dover and A. Gal, Prog. Part. Nucl. Phys. **12**, 171 (1985).
[26] J. Schaffner, C. B. Dover, A. Gal *et al.*, Ann. Phys. (NY) **235**, 35 (1994).
[27] D. J. Millener, C. B. Dover, and A. Gal, Phys. Rev. C **38**, 2700 (2001).
[28] T. A. Rijken, M. M. Nagels, and Y. Yamamoto, Prog. Theor. Phys. Suppl. **185**, 14 (2010).
[29] J. J. de Swart, Rev. Mod. Phys. **35**, 916 (1963); **37**, 326 (1965).
[30] T. A. Rijken, V. G. J. Stoks, and Y. Yamamoto, Phys. Rev. C **59**, 21 (1999).
[31] S. Weissenborn, D. Chatterjee, and J. Schaffner-Bielich, Phys. Rev. C **85**, 065802 (2012); Nucl. Phys. A **881**, 62 (2012).
[32] J. R. Oppenheimer and G. M. Volkoff, Phys. Rev. **55**, 374 (1939).
[33] R. C. Tolman, Proc. Natl. Acad. Sci. USA **20**, 169 (1934).
[34] J. M. Lattimer and M. Prakash, Phys. Rep. **621**, 127 (2016).
[35] G. Baym, C. Pethick, and P. Sutherland, Astrophys. J. **170**, 299 (1971).
[36] E. E. Flanagan and T. Hinderer, Phys. Rev. D **77**, 021502(R) (2008).
[37] T. Hinderer, Astrophys. J. **677**, 1216 (2008)
[38] S. Postnikov, M. Prakash, and J. M. Lattimer, Phys. Rev. D **82**, 024016 (2010).
[39] T. Hinderer, B. D. Lackey, R. N. Lang, and J. S. Read, Phys. Rev. D **81**, 123016 (2010).
[40] U. Garg and G. Colò, Prog. Part. Nucl. Phys. **101**, 55 (2018).
[41] C. Providencîa and A. Rabhi, Phys. Rev. C **87**, 055801 (2013).
[42] H. Takahashi *et al.*, Phys. Rev. Lett. **87**, 212502 (2001).
[43] J. K. Ahn *et al.*, Phys. Rev. C **88**, 014003 (2013).
[44] M. Fortin, S. S. Avancini, C. Providencîa, and I. Vidaña, Phys. Rev. C **95**, 065803 (2017).
[45] L. Lopes and D. Menezes, J. Cosmol. Astropart. Phys. 05 (2018) 038.
[46] T. Miyatsu, T. Katayama, and K. Saito, Phys. Lett. B **709**, 242 (2012).

[47] B. G. Todd-Rutel and J. Piekarewicz, Phys. Rev. Lett. **95**, 122501 (2005).
[48] M. Dutra, O. Lourenço, and D. P. Menezes, Phys. Rev. C **93**, 025806 (2016)
[49] O. Lourenço, M. Dutra, C. H. Lenzi, C. V. Flores, and D. P. Menezes, Phys. Rev. C **99**, 045202 (2019).
[50] L. L. Lopes and D. P. Menezes, Phys. Rev. C **89**, 025805 (2014).
[51] R. O. Gomes, V. Dexheimer, S. Schramm, and C. A. Z. Vasconcellos, Astrophys. J. **808**, 8 (2015).
[52] P. Krastev and B.-A. Li, J. Phys. G (2019), doi:10.1088/1361-6471/ab1a7a.
[53] A. T. Rijken and H. J. Schulze, Eur. Phys. J. A **52**, 21 (2016).
[54] T. B. Gross, C. Fuchs, and A. Faessler, Nucl. Phys. A **648**, 105 (1999).
[55] K. Yagi and N. Yunes, Phys. Rev. D **88**, 023009 (2013).
[56] K. Yagi, L. C. Stein, G. Pappas, N. Yunes, and T. A. Apostolatos, Phys. Rev. D **90**, 063010 (2014).
[57] J. B. Wei, A. Figura, G. F. Burgio, H. Chen, and H. J. Schulze, J. Phys. G **46**, 034001 (2019).
[58] C. Breu and L. Rezzolla, Mon. Not. R. Astron. Soc. **459**, 646 (2016).